Field Measurements of Natural and Artificial Targets Using a Mid-Infrared Laser Reflectance Sensor

Ram M. Narayanan, *Senior Member, IEEE*, and Steven E. Green

***Abstract*—A tunable mid-infrared CO_2 laser reflectance sensor operating in the 9–11 μm wavelength range has been developed and field-tested at the University of Nebraska. This system is capable of gathering reflectance data at various wavelengths, incidence angles and linear polarization combinations. Preliminary measurements of various natural and artificial targets such as soil, coniferous and deciduous trees, concrete and brick building material at distances of up to 100 m demonstrate the potential of this system to characterize the mid-infrared reflectance of terrain features for remote sensing applications. Field-acquired data compare well with data on similar materials measured in the laboratory under controlled conditions.**

I. Introduction

THE study of the mid-infrared (mid-IR) reflectance of terrestrial materials has been motivated by applications such as remote sensing of terrestrial lithology [1], and calibration of downward-looking differential-absorption lidar (DIAL) sensors aboard aircraft or spacecraft [2], [3]. Airborne CO_2 laser spectrometer systems have been used recently for making reflectance measurements over various terrain targets [4]–[7]. The University of Nebraska has studied the CO_2 laser reflectance characteristics of various natural and artificial materials under controlled laboratory conditions [8], [9]. These data provided some indication of the spectral characteristics of various types of targets, as well as quantitative comparisons of the mid-IR reflectance between these materials. The next step was to characterize some of these targets under field-type conditions, wherein the inhomogeneities within the illuminated spot size, as well as the variations due to the intervening atmosphere can be significant.

II. Sensor Description

The University of Nebraska line-tunable CO_2 laser reflectance sensor system is designed to gather reflectance data at various wavelengths, incidence angles and linear polarization combinations. It consists of a Laser Photonics CL75-STVO tunable CO_2 waveguide laser, an EG&G Judson J15D12 cryostat-cooled HgCdTe detector/preamplifier, a Stanford Research Systems SR 530 Dual-phase lock-in amplifier, and supporting optics. The laser is linearly polarized and water-cooled and operates in the TEM_{oo} mode with a minimum output power of 5.5 W over the tunable 9–11 μm wavelength range, a FWHM gain linewidth of 425 MHz, and a beam divergence of 8 mrad. Its output polarization purity was quoted as better than 600:1. A 50/50 beamsplitter in the laser output beam directs one-half the energy to the target, and the other half into a power meter. The detector with a 0.25 mm square active size, a typical responsitivity of 5 mV/μw, a minimum D^* of 3×10^{10} cm $Hz^{1/2}$ W^{-1} at 20 kHz and 60° FOV, is followed by a matched preamplifier of voltage gain equal to 500. A 15-mm focal length lens is used to focus the beam onto the detector, and its f/D ratio is unity. The FOV of the lens-detector combination is approximately 17 mrad, thus enabling full capture of the laser beam. The lock-in amplifier has 100 nV full scale sensitivity and 6 nV $Hz^{-1/2}$ typical input noise at 1 kHz. A 10,000:1 extinction ratio polarizer is used before the receiver lens to select co-polarized or cross-polarized backscattered energy.

A block diagram of the system configuration is shown in the Fig. 1. Various other accessories shown are used for instrument control, data storage and hardcopy outputs. The entire optical system including the bottle containing the pressurized nitrogen gas for the cryostat is enclosed in a box. For a target depolarization ratio of 0.1, the error in our cross-polarized reflectance and depolarization ratio values is estimated as approximately 20%, due to the imperfect polarization purity of the outgoing beam. Calculations based on our prior laboratory measurements indicate that low-level cross-polarized backscattered signals can be measured at distances of up to 100 m with a signal-to-noise (S/N) ratio of better than 10 dB. The system was optimized for operation at a range of 20 m.

III. Measurement Results

The field measurements were performed at twelve wavelengths in the 9–11 μm range, as listed in Table I. The laser output power was constantly monitored using the power meter. A list of targets measured in the field is shown in Table II. Calibration was accomplished using a 45.72-cm × 45.72-cm square Infragold Diffuse Reflectance Standard of 94% nominal reflectance [10].

For stationary targets, such as the calibration standard, soil, concrete and brick, spatial averaging was performed by physically illuminating four different spots on the targets. For vegetative targets, motion due to wind-action provided adequate temporal averaging for each measurement. The receiving system Fresnel number, N, is obtained from the expression [7]

$$N = \frac{D(\mathrm{FOV})}{4\lambda}$$

Manuscript received February 2, 1994; revised May 19, 1994.

The authors are with the Deptartment of Electrical Engineering/Center for Electro-Optics, University of Nebraska, Lincoln, Nebraska 68588-0511 USA.

IEEE Log Number 9403613.

1041-1135/94$04.00 © 1994 IEEE

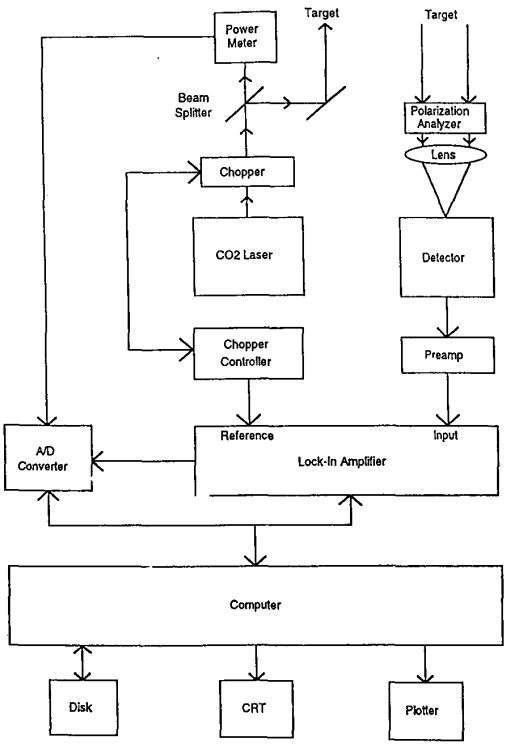

Fig. 1. Block diagram of laser reflectance sensor.

TABLE I
WAVELENGTHS FOR FIELD MEASUREMENTS

S.No.	Line	Wavelength (μm)
1	R(34)	9.2010
2	R(24)	9.2500
3	R(18)	9.2825
4	P(16)	9.5195
5	P(22)	9.5690
6	P(30)	9.6395
7	R(30)	10.1825
8	R(20)	10.2470
9	R(10)	10.3190
10	P(10)	10.4945
11	P(20)	10.5915
12	P(24)	10.6325

where D is the telescope aperture, FOV is the receiver field of view and λ is the wavelength. For $D = 15$ mm, FOV $\simeq 17$ mrad and $\lambda = 10$ μm, we obtain $N = 6.25$. This quantity is the number of uncorrelated speckle samples in each measurement. Since four spatial samples were incoherently averaged in the case of stationary targets, the "effective" Fresnel number is given by the product of 6.25 and $\sqrt{4}$, which is 12.5. The depth of modulation due to speckle, which is inversely proportional to the "effective" Fresnel number, is computed as $\pm 4\%$. For vegetative targets, wind action causes the leaves and needles to flutter, resulting in a large number of independent realizations of the random scattering process. The number of independent samples is estimated as the ratio of the total observation time to the decorrelation time. We estimate this number to be large ($\sim$100), thus resulting in an "effective" Fresnel number of 62.5 and a depth of modulation of $\pm 0.8\%$ for our vegetation measurements. Averaged data for the calibration target are plotted in Fig. 2, with intensity (in V/W) on the Y-axis and wavelength on the X-axis. Intensity is defined as the ratio of the detected voltage to the transmitted laser power, thereby accounting for the power output variations of the laser as a function of time as well as wavelength. Although this definition appears arbitrary, it can be used to directly calculate the target reflectance if the transfer functions of the optical and the electronic components are accurately known. Calibration measurements were made at an incidence angle of 30°, since not only was the reflected power at normal incidence very aspect sensitive, due to partly specular behavior at 0° incidence, but also because the normal incidence reflected power was large enough to saturate the detector. The reflectance characteristics are, as expected, generally flat over the wavelength range, although variations of the order of $\pm 10\%$ are seen. It should be noted that these values represent a spatial average of only 12.5 independent measurements, which explains the large variability.

TABLE II
LIST OF TARGETS INVESTIGATED

S.No.	Target Type	Approximate Range (m)
1	Clay Brick/Mortar	20
2	Decorative Concrete	100
3	Concrete	20
4	Soil	20
5	Cottonwood Tree	20
6	Austrian Pine Tree	20
7	Red Pine Tree	30

Similar data were obtained on other target types. We also attempted to calibrate these data sets in terms of their normalized reflectance. The normalized reflectance is defined as the ratio of the power (or intensity) reflected from the target at the specific incidence angle and polarization to the co-polarized power reflected at normal incidence from the calibration standard placed at the same range as the target under consideration. The normalized reflectance of the target, ρ, was obtained using the expression

$$\rho = R_\theta \left(\frac{I_t}{I_c}\right)\left(\frac{d_t}{d_c}\right)^2$$

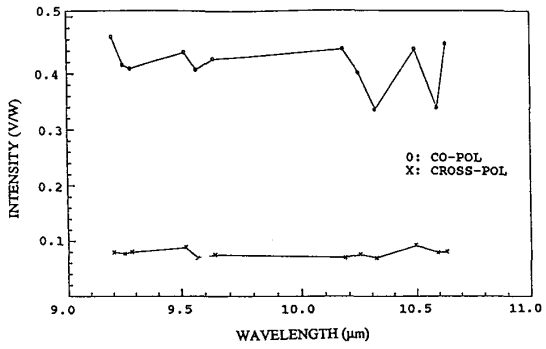

Fig. 2. Reflectance characteristics of calibration standard.

where I_t and I_c are the intensities (in V/W) reflected from the target and the calibration standard respectively, d_t and d_c are the distances to the target and the calibration standard, and R_θ is the ratio of the intensity reflected from the calibration target at the specified incidence angle (30° in our case) to that reflected at normal incidence, which accounts for the normalization to normal-incidence co-polarized reflectance from the calibration standard. At 30° incidence, this value was measured as 0.17 using a precision scatterometer. The squared term in the above expression accounts for the spreading factor. Although the above expression is exact, uncertainties in d_t and d_c will ultimately limit the quantitative accuracy of the computed reflectance values. The following plots of the reflectance characteristics show both the measured intensities as well as the computed normalized reflectances on the Y-axis.

Figure 3(a) shows the reflectance characteristics of soil, which had been excavated and piled near a construction site. Although the soil was not analyzed texturally or mineralogically, it is presumed to contain large quantities of quartz. The reflectance characteristics do show the reststrahlen peak in the vicinity of 9-μm. Furthermore, the reflectance near 10.5 μm is almost one-quarter the 9 μm reflectance, consistent with earlier laboratory observations. Data on decorative concrete containing small quartz pebbles of 0.5 to 1 cm size are shown in Figure 3(b), in which the quartz reststrahlen characteristics are clearly seen. Depolarization ratios (ratio of cross-polarized to co-polarized intensities) are of the order of 10% and 16% for soil at the lower and upper band edges respectively, while corresponding values for concrete are approximately 23% and 30%.

Data on two of the trees studied are presented. Figure 4(a) shows the reflectance characteristics of the Cottonwood tree (*Populus Deltoides*), which consists of a broad spreading crown containing relatively smooth leaves that are 7.5–18 cm long and 7.5–13 cm wide. The reflectance characteristics are flat and featureless over the wavelength band, and show no significant depolarization, which can be attributed to the specular leaf surfaces. The Austrian Pine tree (*Pinus Nigra*), on the other hand, is a densely foliated coniferous tree containing evergreen needles 9–15 cm long. Its reflectance characteristics, shown in Figure 4(b), also demonstrate flat features with respect to wavelength, and significantly higher depolarization (~5%) compared to the Cottonwood tree.

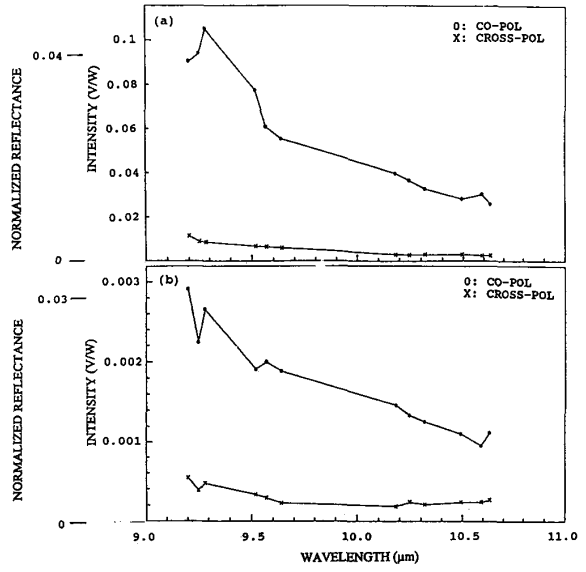

Fig. 3. Reflectance characteristics of (a) soil and (b) decorative concrete.

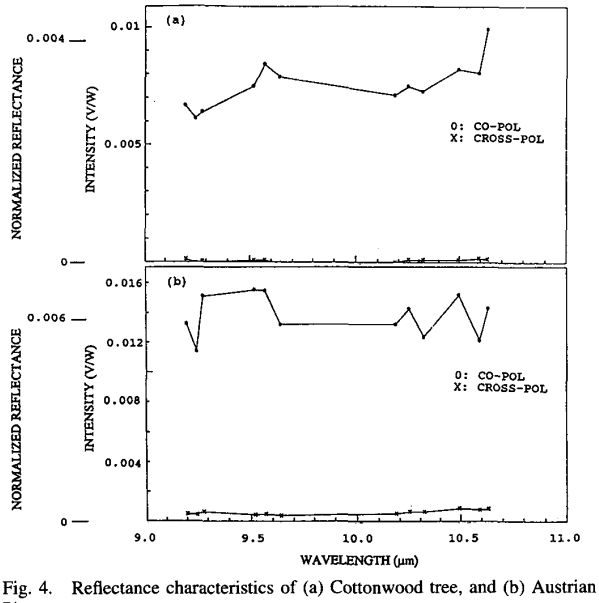

Fig. 4. Reflectance characteristics of (a) Cottonwood tree, and (b) Austrian Pine tree.

These preliminary results demonstrate the ability of our CO_2 laser reflectance sensor to acquire co-polarized and cross-polarized backscatter from terrestrial targets under field conditions. Data obtained are consistent with our earlier controlled laboratory investigations.

REFERENCES

[1] J. E. Eberhardt, J. G. Haub, and A. W. Pryor, "Reflectivity of natural and powdered minerals at CO_2 laser wavelengths," *Appl. Opt.*, vol. 24, no. 3, pp. 388–395, 1985.

[2] M. S. Shumate, S. Lundquist, U. Persson, and S. T. Eng, "Differential reflectance of natural and man-made materials at CO_2 laser wavelengths," *Appl. Opt.*, vol. 21, no. 13, pp. 2386–2389, 1982.

[3] W. B. Grant, "Effect of differential spectral reflectance on DIAL measurements using topographical targets," *Appl. Opt.*, vol. 21, no. 13, pp. 2390–2394, 1982.

[4] K. Wiesemann, R. Beck, W. Englisch, and K. Gurs, "In-flight test of a continuous laser remote sensing system," *Appl. Phys.*, vol. 15, no. 3, pp. 257–260, 1978.

[5] J. L. Bufton, T. Itabe and D. A. Grolemund, "Dual-wavelength correlation measurements with an airborne pulsed CO_2 laser system," *Opt. Lett.*, vol. 7, no. 12, pp. 584–586, 1982.

[6] A. B. Kahle, M. S. Shumate, and D. B. Nash, "Active airborne infrared laser system for identification of surface rock and minerals," *Geophy. Resear. Lett.*, vol. 11, no. 11, pp. 1149–1152, 1984.

[7] L. B. Whitbourn, R. N. Phillips, G. James, M. T. O'Brien, and M. D. Waterworth, "An airborne multiline CO_2 laser system for remote sensing of minerals," *J. of Modern Opt.*, vol. 37, no. 11, pp. 1865–1872, 1990.

[8] R. M. Narayanan, S. E. Green, and D. R. Alexander, "Mid-infrared backscatter spectra of selected agricultural crops," *Proc. SPIE Symp. on Opt. in Agriculture*, eds. J. A. DeShazer and G. E. Meyer, (Boston, MA), vol. 1379, Nov. 1990, pp. 116–122.

[9] R. M. Narayanan, S. E. Green, and D. R. Alexander, "Mid-infrared backscatter characteristics of various benchmark soils," *IEEE Transactions on Geosci. Remote Sensing*, vol. 30, no. 3, pp. 516–530, 1992.

[10] R. W. Willey, "Results of a round robin measurement of spectral emittance in the mid-infrared," *Proc. SPIE Symp. on Passive Infrared Systems and Technology*, ed. H. Lamberton, vol. 807, 1987, pp. 140–147.